

OPTIMIZING THE ROTHERMEL MODEL FOR EASILY PREDICTING SPREAD RATE OF FOREST FIRE

J. HUA¹, S. ZHANG^{1*}, H. GAO¹, X. CHEN¹, X. LI^{1,2*}, J. LIU^{1*}

¹ College of Mechanical and Electrical Engineering, Northeast Forestry University, Harbin 150040, China;

² Northern Forest Fire Management Key Laboratory of the State Forestry and Grassland Bureau,
Northeast Forestry University, Harbin Harbin 150040, China

*Corresponding Author

ABSTRACT. The Rothermel model is a common method for predicting forest fire spread rate, but its application is limited, due to the complexity of the formula and too many parameters. In this paper, the Rothermel model is optimized to a simpler format, which contains fuel moisture content, wind speed, fuel load, fuel thickness 4 independent variables as input, 1 dependent variable as output and 8 parameters to be estimated. In order to validate the effectiveness of the optimized model, an indoor ignition experiment was designed and carried out, and then the fire spreading data was collected and processed in advance for training the parameters of the model. By analyzing the effectiveness of 3 nonlinear optimizing methods, the Levenberg-Marquardt (*LM*) method was chosen to estimate the parameters of the model. Last, by comparing to the actual measured value, the precision of the optimized model was validated on the verification data which contains three groups of experiments, with the ability to predict quickly the speed of fire spreading compared with the Rothermel model in the indoor laboratory.

Keywords: Rothermel forest fire spread model; fire behavior; nonlinear fitting; prediction of spread rate

1 BACKGROUND

Forests are the protectors of the ecological balance of the earth. Unfortunately, forest fires are usually observed only when they have spread to a large area. At this time, it is impossible to extinguish or control forest fires, resulting in serious damage to property and irreparable damage to the environment (Gigovic et al. 2019). When a forest fire occurs, if firefighters can forecast the development of the disaster as soon as possible and understand the changing trend of the fire, they can seize the initiative, deploy fire fighting forces pertinently, and control the spread of the fire to the greatest extent (Ying et al. 2018). Therefore, it is necessary to study the changing rules and the parameters of forest fires in the process of spread, and use the potential rules between the parameters to establish the related forest fire spreading model, so as to predict the forest fire spreading trend in the real scene (Rossi et al. 2019). It is an intuitive, reliable, economical and efficient prediction method to simulate the development process of real forest fire completely. At present, there is no model

that can accurately describe the forest fire spread trend and the burning state of the complexity of the forest fire and the difference in the burning area (Xue et al. 2015). Among the common forest fire spread models abroad, the Rothermel forest fire spread model is the most representative (Prince et al. 2017), and the Rothermel (Dhall et al. 2017) is a semi-physical and semi-empirical forest fire spread prediction model based on energy conservation, which has strong practicability.

In order to study the influence of wind speed on the spread of forest fire, Lopes (2019) put forward the principle of two-way coupling of wind speed and firepower, and carried out simulation experiments based on Rothermel model to verify the effectiveness of the model. In order to study the influence of input parameters in Rothermel model, Ervilha (2016) carried out experiments in different scenarios and quantified the parameters in the formula. The results support the applicability of NISP method in stochastic calculation of forest fire spread. Zhang (2012) took *Korean pine* and *Quercus mongolica* as mixed combustibles as the research object in the laboratory, simulated the spread rate of forest fire on the

basis of windless flat land. Indoor spot burning experiments with different moisture content, load and mixing ratio were carried out. Observed propagation rate, residence time, reaction intensity, fire line intensity and flame length, was compared with the prediction value of the generalized Rothermel model using surface area weighting method and load weighting method. The results shown that the model obtained by this method had high prediction ability. Taking the dead combustibles on the ground surface as the research object, Man (2019) simulated the spread of forest fire in the laboratory by changing the relevant variables such as the thickness, load and moisture content of the combustion bed. Re-estimated the parameters of Rothermel's forest fire spread by recording the spread speed of combustibles, so as to forecast the combustion state of forest fires using the Rothermel's forest fire spread model after re-estimating the parameters. The experiments in the article shown that the prediction accuracy of the model was good. Yang (2018) made an in-depth analysis and model study on the heat transfer mechanism of downhill fire spread, focused on the relationship between various fire behaviors and slope, the experiments conclusions were consistent with those described in previous literature.

From the above papers, it can be seen that the Rothermel plays an important role in the current stage of forest fire spreading, both models and simulation software require Rothermel as a bridge, however, the complex formula and the relationship between parameters limit its application and development, so it is necessary to simplify the model and evaluate the simplified model. Also, the models of the above scholars have good predictive ability, but the results show that there are certain errors, for example, there are certain errors in the benchmark method and thermocouple method when measuring the line speed. In addition, scholars fail to consider the two key factors of fire spread: wind speed and slope. Therefore, this paper uses the image measurement method with relatively high accuracy (Li et al. 2014) to extract the multi-point spread speed of the fire line. In addition, the wind speed and slope variables are added in the burning experiment to study the simulation of fire spread under multi-variables, simplify the Rothermel spread model, and test its accuracy.

2 EXPERIMENTAL DATA PREPROCESSING

The forest combustibles are a complex mixture, and different trees produce different amounts of combustion energy. The tree species near Maoershan Forest Farm (Geographical coordinates: N45°20'45.25'', E127°30'12.734'') of Northeast Forestry University include coniferous tree species such as *Pinus sylvestris var. mon-*

golica, Korean pine, *Larix gmelinii*, *Picea*, and broad-leaved tree species such as *PopulusL*, *Quercus mongolica*. It is found that *Pinus sylvestris var. mongolica* has strong flammability, poor fire resistance and wide planting area in Maoershan forest area, so *Pinus sylvestris var. mongolica* is used as the experimental object. The indoor burning experiment needs to convert the two-dimensional point coordinates captured by the camera to the three-dimensional point coordinates in the real world. This process requires the perspective transformation.

2.1 Perspective transformation

The size of the combustion bed in the laboratory is 1m*1.5m. A layer of asbestos blanket is placed on the combustion bed for heat insulation. A group of infrared cameras and visible light cameras are placed on the front and rear sides of the combustion bed respectively. A electric fan is placed directly in front of the combustion bed to add a variable of wind speed. The calibration board is to determine the conversion relationship between physical size and pixels. Positional of calibration plate, camera and combustion bed are shown in (Fig. 1). Perspective transformation is the projective transformation of the center projection, which is a fractional linear transformation of the plane when expressed in non-homogeneous projective coordinates. The perspective

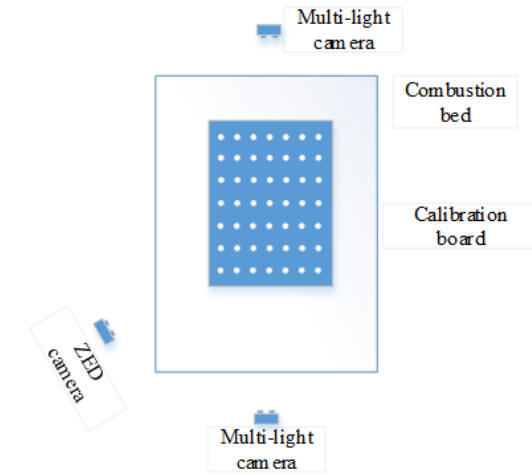


Figure 1: Positional of calibration plate, camera and combustion bed

transformation formula:

$$\begin{bmatrix} X \\ Y \\ Z \end{bmatrix} = \begin{bmatrix} a_{11} & a_{12} & a_{13} \\ a_{21} & a_{22} & a_{23} \\ a_{31} & a_{32} & a_{33} \end{bmatrix} \begin{bmatrix} x \\ y \\ 1 \end{bmatrix} \quad (1)$$

Where

$$\begin{bmatrix} a_{11} & a_{12} & a_{13} \\ a_{21} & a_{22} & a_{23} \\ a_{31} & a_{32} & a_{33} \end{bmatrix}$$

is the Perspective transformation matrix,

$$\begin{bmatrix} x \\ y \\ 1 \end{bmatrix}$$

is coordinates of points on the fire line of the image;

$$\begin{bmatrix} X \\ Y \\ Z \end{bmatrix}$$

is the coordinates of the point on the line of the actual position; The fire spread is on the plane of the combustion bed, so divide the coordinates of the point on the actual fire line by Z :

$$\begin{cases} X' = \frac{X}{Z} \\ Y' = \frac{Y}{Z} \\ Z' = \frac{Z}{Z} \end{cases} \quad (2)$$

simplify:

$$\begin{cases} X' = \frac{a_{11}x + a_{12}y + a_{13}}{a_{31}x + a_{32}y + a_{33}} \\ Y' = \frac{a_{21}x + a_{22}y + a_{23}}{a_{31}x + a_{32}y + a_{33}} \\ Z' = 1 \end{cases} \quad (3)$$

to find X' , Y' four known coordinate points are found on the fire spread plane, that is,

$$\{a_{11}, a_{12}, a_{13}, a_{21}, a_{22}, a_{23}, a_{31}, a_{32}\}$$

eight unknowns are solved. The four corners of the calibration board can be easily identified by the camera, the calibration board is placed on the combustion bed before the experiment, and the coordinates of all the points on the combustion plane can be obtained through the calibration board.

2.2 Calculation of fire spread rate

After knowing the actual location of the fire point, we need to specify the speed calculation method of the fire line. In the process of fire spread (Fig. 2), five points P_1 , P_2 , P_3 , P_4 , P_5 on the fire line L at the initial time, make the tangent of the fire line L respectively through these five points, and then make the tangent line perpendicular to these five points. The intersection of the vertical line and the fire line L' at the next moment in the spreading process is the corresponding spreading point, and the ratio of the distance to time between the corresponding points in the spreading process is the spread speed of the fire line, and the velocities of five points are obtained respectively. Then the average value is the spread speed of the fire line in this period of time (Rossi et al. 2019).

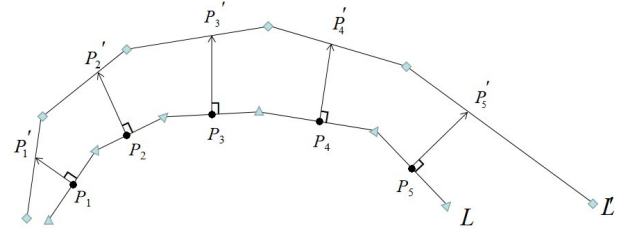


Figure 2: Schematic diagram of fire spreading speed calculation

3 MODEL OPTIMIZATION

3.1 Optimizing the Rothermel forest fire spread model

The Rothermel forest fire spread model has been recognized by scholars at this stage due to its good predictive ability (Pan et al. 2017), but its own parameters need to be input (Ervilha et al. 2016), and the relationship between the spread rate and each parameter cannot be clearly observed. Therefore, it is necessary to simplify the Rothermel model to obtain the nonlinear relationship between independent variables and dependent variables, and then predict the spread of forest fire. As shown in Eq. (4), Rothermel forest fire spread model is:

$$R = \frac{I_R \times \zeta \times (1 + \Phi_W + \Phi_S)}{P_b \times \varepsilon \times Q_{ig}} \quad (4)$$

$$\begin{aligned} I_R = & (0.0591 + 2.926\sigma^{-1.5})^{-1} \left(\frac{\beta}{\beta_{op}} \right)^{8.9033\sigma^{-0.7913}} \\ & \exp \left[8.9033\sigma^{-0.7913} \left(1 - \frac{\beta}{\beta_{op}} \right) \right] [W_0(1 - S_T)] \\ & h \left[1 - 2.59 \frac{M_f}{M_x} + 5.11 \left(\frac{M_f}{M_x} \right)^2 - 3.52 \left(\frac{M_f}{M_x} \right)^3 \right] \\ & (0.174S_E^{-0.19}) \end{aligned} \quad (5)$$

$$\zeta = (192 + 7.9095\sigma)^{-1} \exp[0.792 + 3.7597\sigma^{0.5}](\beta + 0.1) \quad (6)$$

$$\begin{aligned} \Phi_W = & 7.47 \exp(-0.8711\sigma^{0.55})(3.281U)^{0.15988\sigma^{0.55}} \\ & \left(\frac{\beta}{\beta_{op}} \right)^{-0.751 \exp(-0.01094\sigma)} \end{aligned} \quad (7)$$

$$\Phi_S = 5.275\beta^{-0.3} \tan \Phi^2 \quad (8)$$

$$P_b = \frac{W_0}{\delta} \quad (9)$$

$$\varepsilon = \exp\left(\frac{-0.5428}{\sigma}\right) \quad (10)$$

$$Q_{ig} = 581 + 2594M_f \quad (11)$$

Where R is spreading rate, I_R is the reaction intensity, W_0 is drying combustible load, Φ_w is wind speed correction factor, Φ_s is slope correction factor, P_b is drying particle density, Q_{ig} is effective heat coefficient, ε is pre-combustion heat, β is compression ratio, σ is surface area to volume ratio, M_f is moisture content, M_x is combustible extinguishment moisture content, all parameters are in metric units. Sorted out by the above style is shown in Eq. (12):

$$\begin{aligned} R = & h \cdot (1 - S_T) \delta (0.174 S_E^{-0.19}) [(0.0591 + 2.926 \sigma^{-1.5})^{-1} \\ & \cdot (192 + 7.9095 \sigma)^{-1} \left(\frac{\beta}{\beta_{op}} \right)^{8.9033 \sigma^{-0.7913}}] \\ & \exp [8.9033 \sigma^{-0.7913} \cdot (1 - \frac{\beta}{\beta_{op}}) + (0.792 + 3.7597 \sigma^{0.5}) \\ & (\beta + 0.1) + \frac{0.5428}{\sigma}] \\ & [1 + 1.747 \exp(-0.8711 \sigma^{0.55}) (3.281 U)^{0.1598 \sigma^{0.55}} \\ & \left(\frac{\beta}{\beta_{op}} \right)^{-0.751} \exp(-0.01094 \sigma) + 5.275 \beta^{-0.3} (\tan \Phi)^2] \\ & \left[\frac{1 - 2.59 \frac{M_f}{M_x} + 5.11 (\frac{M_f}{M_x})^2 - 3.52 (\frac{M_f}{M_x})^3}{581 + 2954 M_f} \right] \end{aligned} \quad (12)$$

For combustibles of the same material, surface area to volume ratio σ , low heat content h , total mineral content S_T , effective mineral content S_E are all fixed values compression ratio β is:

$$\beta = \frac{P_b}{P_p} = \frac{W_0}{\delta P_p} \quad (13)$$

The density of dried particles P_b is also constant for the same kind of combustibles,

$$\beta_{op} = 0.20395 \sigma^{-0.8189} \quad (14)$$

so Eq. (12) can still be simplified as Eq. (15):

$$\begin{aligned} R = & B \delta \left(K \frac{W_0}{\delta} \right)^C \exp [C \cdot (1 - K \frac{W_0}{\delta}) \\ & + E \left(K \frac{W_0}{\delta} + 0.1 \right) f(m)] \\ & [1 + G U^H \left(K \frac{W_0}{\delta} \right) I + J \left(\frac{W_0}{\delta} \right)^{-0.3} (\tan \Phi)^2] \end{aligned} \quad (15)$$

where

$$\begin{aligned} B = & h \cdot (1 - S_T) (0.174 S_E^{-0.19}) [(0.0591 + 2.926 \sigma^{-1.5})^{-1} \\ & \cdot (192 + 7.9095 \sigma)^{-1}] \end{aligned} \quad (16)$$

$$C = 8.9033 \sigma^{-0.7913} \quad (17)$$

$$E = 0.792 + 3.7597 \sigma^{0.5} \quad (18)$$

$$f(m) = \frac{1 - 2.59 \frac{M_f}{M_x} + 5.11 (\frac{M_f}{M_x})^2 - 3.52 (\frac{M_f}{M_x})^3}{581 + 2954 M_f} \quad (19)$$

$$G = 1.747 \exp(-0.8711 \sigma^{0.55}) \cdot (3.281^{0.1598 \sigma^{0.55}}) \quad (20)$$

$$H = 0.1598 \sigma^{0.55} \quad (21)$$

$$I = -0.751 \exp((0.01094 \sigma)) \quad (22)$$

$$J = 5.275 P_b^{-0.3} \quad (23)$$

$$K = \frac{1}{P_b (0.20359 \sigma^{-0.8198})} \quad (24)$$

In the optimized Rothermel forest fire spread model, B , C , E , G , H , I , J , K are the parameters to be estimated, while The combustible bed depth δ , the drying combustible load W_0 , the flame central wind speed U , the slope Φ , the combustible moisture content M_f , the combustible extinguishment moisture content M_x are independent variables, and $f(m)$ is a function containing M_f and M_x . In order to obtain the parameters of the function to be estimated in the optimized forest fire spread model, it is necessary to measure the numerical changes of independent variables and dependent variables with flame spread.

3.2 Experimental method

In order to explore the relationship between model parameters after optimization, we conduct experiments. During the experiment, varying the thickness of each of the fuel bed, the surface area of fuel, fuel drying mass, the combustion bed and the outside slope of wind speed. The moisture content of combustibles is measured by the ratio of fresh weight to dry weight and fresh weight, in which the dry weight is the quality after collecting leaves and drying in the oven for 30 hours, and the fresh weight is the quality after natural moisture regain. The

flame central wind speed measures the real-time flame central wind speed by following the flame spread with a hand-held anemograph. The thickness of the bed is determined by measuring the average thickness of multiple combustible beds, and the bed inclination angle of the combustion bed is measured by a level meter.

Tab. 1 shows the setting of the parameters of the experiment, in which the quantity is divided into four grades: 0.6kg, 0.7kg, 0.9kg and 1.2kg, and the surface integral is divided into 0.8*0.6m², 1.0*0.6m² and 1.0*0.4m², the combustible bed thickness is divided into 0.04mm, 0.06mm, 0.08mm three grades, the moisture content is divided into 5%, 7%, 10% (moisture content can not be artificially controlled, can only be controlled moistureproof time is roughly divided into three grades), the inclination is divided into 0 °, 8 °, 18°, the wind speed of the electric fan is divided into 1 wind level, 2 wind level, 3 wind level. The 13 groups of experiments are divided into training data set and verification data set, and the sequence numbers 6, 7 and 10 are randomly selected as the verification data set according to the proportion of 20%.

3.3 Solving Optimized model parameters

Firstly, the training data sets are used to solve the parameters of the model. The solution of model parameters is a mathematical method to estimate the parameters of optimized Rothermel model through several groups of experimental data on the basis of mathematical theory and empirical understanding of Rothermel model (Rios et al. 2016). The common parameter solving methods are steepest descent method, Newton method, Conjugate Gradient method and Levenberg-Marquardt (*LM*) method (Ding et al. 2014). The fitting effect of parameters is often judged by the following indexes (Zhang et al. 2012): (1) Coefficient of determination. The definable coefficient represents the numerical characteristics of the relationship between a random variable and multiple random variables, and is a statistical indicator used to reflect the reliability of the regression model to explain the change of the dependent variable. (2) Sum of squares of residuals. Statistically, the difference between the data point and its corresponding position on the regression line is called residual, and each residual squared is called the sum of residual sum of residual squares of a group of data is, the better the fitting degree is. (3) Mean square square error. The mean square deviation reflects the degree of dispersion between individuals within a group. In simple terms, the standard deviation is a measure of the degree of dispersion of the average value of a group of data. A larger standard deviation means that there is a

great difference between most values and their average values, and vice versa. (4) Chi-square coefficient. The chi-square test is the degree of deviation between the actual observation value of the statistical sample and the theoretically inferred value. If the chi-square value is the deviation between the two is greater; otherwise, the deviation between the two is smaller. (5) Root mean square error. The root mean square error is the square root of the ratio of the square of the deviation between the predicted value and the real value to the number of observations. It can be seen from the Tab. 2 that the evaluation coefficients of the *LM*'s coefficient of determination, the sum of squared residuals, the mean square error, the root mean square error and the chi-square coefficient are better than other Newton methods and conjugate gradient methods (Brun et al. 2017). In Tab. 2, *LM* is Levenberg-Marquardt method, *Newton* is Newton method, *CG* is Conjugate Gradient method.

It shows the fitting effect of the speed of the optimized Rothermel spread model using the *LM* method (Fig. 3). The horizontal axis represents the serial number of the experimental data, the vertical axis represents the spread speed, the orange line represents the measured value, and the blue line represents the fitting value. It can be clearly seen that except for several extreme points, the blue line fitted by *LM* method can well describe the blue measurement value. The fitted curve can well reflect the actual measured value.

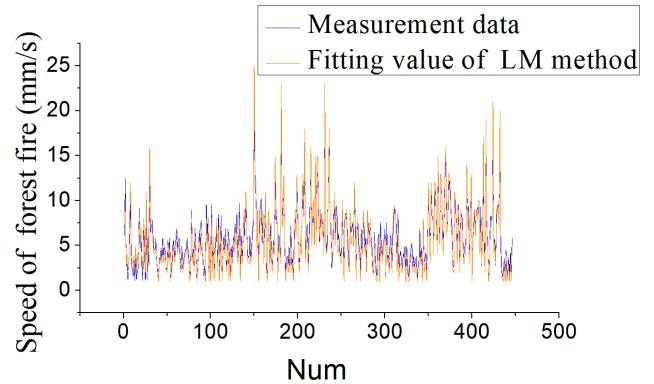


Figure 3: Fitting effect diagram by *LM* method

The eight parameters to be estimated by *LM* method are shown in Tab. 3.

3.4 Model error analysis

Finally, The verification data sets are used to verify the parameters obtained from the training data set. In order to verify the accuracy of the optimized Rothermel forest fire spread model, this paper compares the error between the predictive value of and the measured value (Li et al. 2020). The actual measured value of the veri-

Table 1: Experimental variable settings

Number	Quantity (kg)	surface area (m^2)	bed thickness (m)	inclination (°)	water content (%)	wind speed
1	0.737	1.0*0.6	0.06	8	4.46	3 level
2	0.700	0.8*0.6	0.06	18	4.46	1 level
3	0.725	0.8*0.6	0.08	8	6.79	3 level
4	0.737	1.0*0.4	0.04	18	3.85	3 level
5	1.222	1.0*0.6	0.08	8	11.00	3 level
6	0.548	0.8*0.6	0.04	0	9.52	3 level
7	0.881	0.8*0.6	0.06	0	9.52	2 level
8	0.722	0.8*0.6	0.06	8	7.39	2 level
9	0.945	0.8*0.6	0.06	8	7.39	2 level
10	0.601	0.8*0.6	0.04	18	5.81	2 level
11	0.655	0.8*0.6	0.06	0	5.81	1 level
12	0.692	0.8*0.6	0.06	0	5.24	1 level
13	1.007	0.8*0.6	0.08	18	5.24	1 level

Table 2: Evaluation index of each algorithm

Algorithm	coefficient of determination	Mean square error	Sum of squares of residuals	Chi-square coefficient	Root mean square error
<i>LM</i>	0.901	0.416	77.15	8.42	1.26
Newton	0.863	0.495	109.36	11.99	2.72
<i>CG</i>	0.863	0.495	109.36	11.99	2.71

Table 3: The eight parameters to be estimated by *LM* method

B	K	C	E	H	I	J	G
35.61	0.011	8.86	-29.29	0.2074	6522	412855	7831

fication data, the optimized Rothermel model predicted value are shown (Fig. 4, 5, 6). In mathematical statistics, standard residual refers to the difference between the actual observed value and the estimated value. It can be seen from the standard residual that the residual value is distributed between -0.7 to 0.7, -2 to 2, -0.6 to 0.6, the scattered points are evenly scattered on both sides of the X axis, the optimized model is reliable.

The errors can be obtained by analyzing each verification data as shown in Tab. 4. *ARE* is average relative error, *Max – ARE* is maximum average relative error, *Min – ARE* is minimum average relative error, *AAE* is average absolute error, *Max – AAE* is maximum average absolute error, *Min – AAE* is minimum average absolute error.

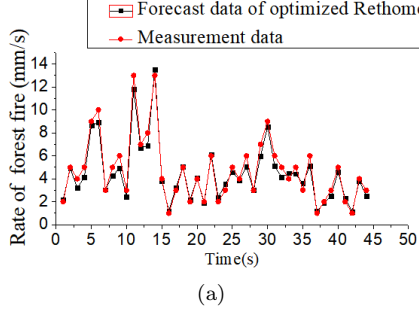
The verification data 1 (No. 7 in Tab. 1) is the inclination of the combustion bed at 0 degrees, the quantity is 0.881kg, the wind of electric fan is 2 level, the water content is 9.52%. The average relative error of the verification data 1 is 10.78%, and the maximum relative error

is 19.67%, the minimum relative error is 1.80%, the average absolute error is 0.47mm/s, the maximum absolute error is 0.89mm/s, and the minimum absolute error is 0.09mm/s. The verification data 2 (No. 6 in Tab. 1) is 0 degree inclination of the combustion bed, the quantity is 0.548kg, the wind of electric fan is 3 level, water content is 9.52%. The average relative error of verification data 2 is 11.94%, the maximum relative error is 19.09%, the minimum relative error is 1.43%, the average absolute error is 0.83mm/s, the maximum absolute error is 0.9mm/s, the minimum absolute error is 0.1mm/s. The verification data 3 (No. 10 in Tab. 1) is the 18-degree inclination of the combustion bed, the quality is 0.601kg, the wind of electric fan is 2 level, and the water content is 5.81%. The average relative error of the verification data 3 is 12.12%, the maximum relative error is 21.67%, the minimum relative error is 5.00%, the average absolute error is 1.25mm/s, the maximum is 2.1mm/s, the minimum absolute error is 0.6mm/s.

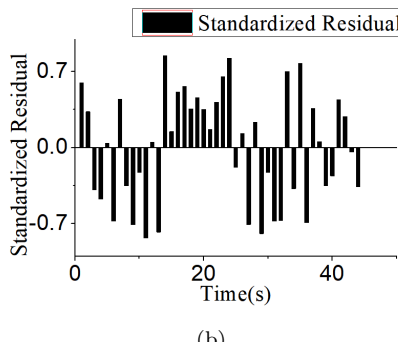
It can be seen that the Rothermel forest fire spread model with re-estimated parameters has the best effect on predicting the forest fire spread speed on the flat ground, while the prediction effect of the forest fire spread under the influence of wind speed and slope decreases, and it can still better predict the forest fire spread speed. Compared with the Rothermel forest fire

Table 4: Error analysis of verification dataset

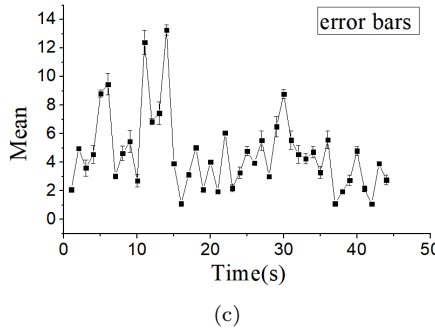
Number	ARE	Max- ARE	Min- ARE	AAE (mm/s)	Max- AAE (mm/s)	Min- AAE (mm/s)
1	10.78%	19.67%	1.80%	0.47	0.8	0.1
2	11.94%	19.09%	1.43%	0.83	0.9	0.1
3	12.12%	21.67%	5.00%	1.25	2.1	0.6



(a)



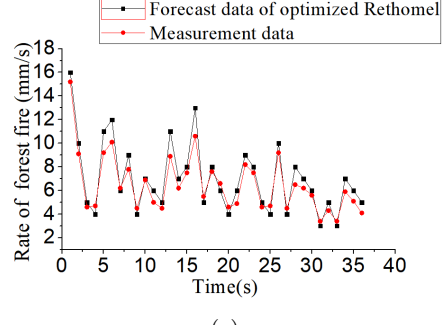
(b)



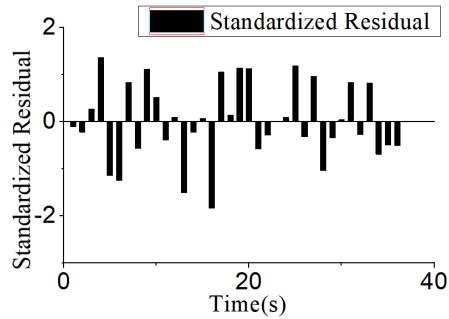
(c)

Figure 4: (a) Comparison of the measured value of verification data 1, the predicted value of optimized Rothermel model; (b) Standard Residual of verification data 1; (c) error bars of verification data 1

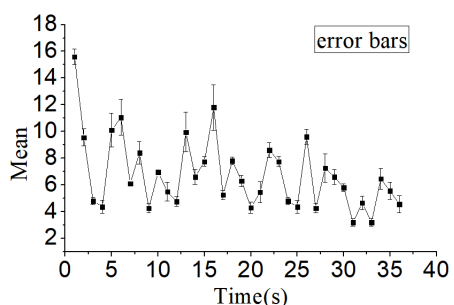
spread model, the optimized Rothermel forest fire spread model is more convenient, and the accuracy can be kept at more than 80%.



(a)



(b)



(c)

Figure 5: (a) Comparison of the measured value of verification data 2, the predicted value of optimized Rothermel model; (b) Standard Residual of verification data 2; (c) error bars of verification data 2

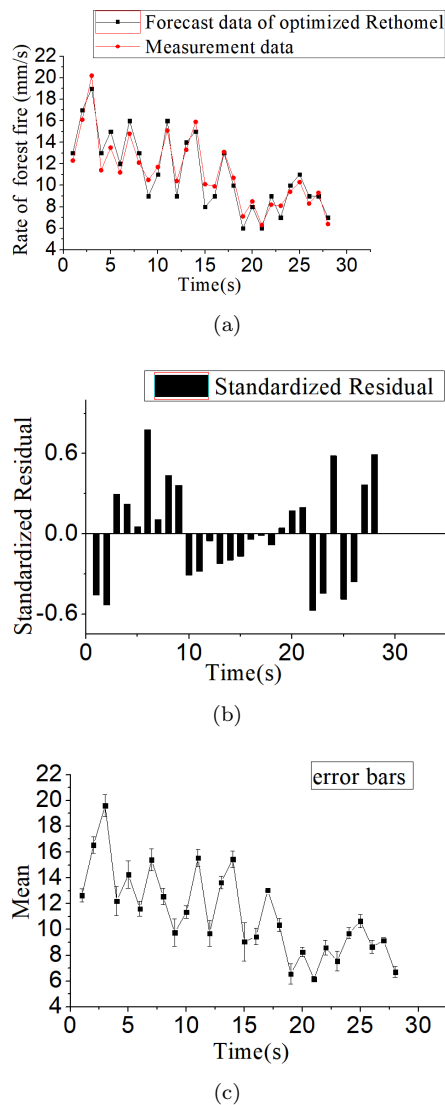


Figure 6: (a) Comparison of the measured value of verification data 3, the predicted value of optimized Rothermel model; (b) Standard Residual of verification data 3; (c) error bars of verification data 3

4 CONCLUSIONS

In this paper, it is found that Rothermel forest fire spread model needs many parameters, complicated formulas and large amount of calculation. Based on the derivation formula and sub-formula of Rothermel forest fire spread model, the original Rothermel forest fire spread model is simplified to a multivariate nonlinear model with four independent variables, such as slope, moisture content, load, wind speed, one dependent variable, such as spread speed, and eight parameters to be estimated. In order to achieving 8 parameters to be estimated, the indoor spot burning experiment is de-

signed. By changing the independent variables such as fuel moisture content, initial spread velocity, combustion bed slope and fuel load, 13 groups of experiments are designed to obtain more than 400 sets of data, including independent variables, dependent variables. This paper analyzes the experimental error in the previous experiment, discards the conventional benchmark method in calculating the fire spread speed of the dependent variable, and uses the method of image processing to calculate the speed of fire spread, which is simple and fast and improves the accuracy of the experimental data. In order to find the law between the data, the data are divided into training data and verification data, and the training datas are substituted into the common nonlinear fitting methods such as Levenberg-Marquardt method, gradient descent method and Conjugate Gradient method, and the indicator parameters of the three nonlinear fitting methods are measured, the results show that the effect of Levenberg-Marquardt method fitting is the best, and 8 parameters to be evaluated by Levenberg-Marquardt method are obtained as the optimized Rothermel forest fire spread model parameters, the spread speed of optimized Rothermel model is obtained by the verification data. It is concluded that the forest fire spread speed predicted by the optimized Rothermel forest fire spread model has an average relative error of 10.78%-12.12% and an average relative error of 0.47-1.25mm/s. The optimized Rothermel forest fire spread model is not only convenient for calculation, the accuracy of prediction is more than 80%.

Because of the complexity of fire behavior, more work needs to be done in the later stage. In addition, the uniformity of combustible materials in the bed is also an important factor affecting the simulation effect of the model, which needs to be regulated in future research to reduce the interference of influencing factors as much as possible. The combustion characteristics of each kind of combustibles are different, which leads to different combustion states, so it is concluded that the parameters to be estimated are different, and the model obtained by a kind of combustibles can not be used as a unified reference formula. Therefore, more models of combustibles should be verified in the later work, and the comparison with other models should be strengthened step by step to prepare for the later burning experiment in the field.

ACKNOWLEDGEMENT

Thanks are due the meticulous comments made by several experts during the peer-review process to make this article more complete. Funding for this study has been supported by “the Fundamental Research Funds for the Central Universities, No. 2572019AB22”, and

"Natural Science Foundation of Heilongjiang Province of China (Grant No. TD2020C001)".

REFERENCES

- Dhall, A., Dhasade, A., Nalwade, A., and Kulkarni, V. 2020. A survey on systematic approaches in managing forest fires. *Applied geography*, 121:102266. DOI: 10.1016/j.apgeog.2020.102266
- Brun, C., Artés, T., Cencerrado, A., Margalef, T., and Cortés, A. 2017. A high performance computing framework for continental-scale forest fire spread prediction. *Procedia Computer Science*, 108:1712-1721. DOI:10.1016/j.procs.2017.05.258.
- Ding Z., Song K., Wang Z. 2014. Ontrastive analysis of algorithms of the forest fire spreading simulation based on Arc GIS Engine. *Journal of University of Chinese Academy of Sciences*. 31(5):640-646. DOI: 2095-6134(2014)05-0640-07.
- Ervilha, A. R., Pereira, J. M. C., and Pereira, J. C. F. 2017. On the parametric uncertainty quantification of the Rothermel's rate of spread model. *Applied Mathematical Modelling*, 41:37-53. DOI: 10.1016/j.apm.2016.06.026.
- Gigović, L., Pourghasemi, H. R., Drobnjak, S., and Bai, S. 2019. Testing a new ensemble model based on SVM and random forest in forest fire susceptibility assessment and its mapping in Serbia's Tara National Park. *Forests*, 10(5):408. <https://doi.org/10.3390/f10050408>.
- Lopes, A.M.G., Ribeiro, L.M., Viegas, D.X., and Raposo, J.R. 2019. Simulation of forest fire spread using a two-way coupling algorithm and its application to a real wildfire. *Journal of Wind Engineering and Industrial Aerodynamics*, 193:103967. DOI: 10.1016/j.jweia.2019.103967.
- Li, D., and Jin, J. 2104. Study on errors of forest re-spread rate measured by visible light image method. *Journal of Central South University of Forestry and Technology*. 34(3):61-67.
- Li, X., Gao, H., Han, C., Wang, Y., Hu, T., Sun, L., and Guo, Y. (2020). An optimized model for predicting forest fires area based on binocular vision. *Mathematical and Computational Forestry & Natural-Resource Sciences (MCFNS)*, 12(1):16-25. Retrieved from <http://mcfns.net/index.php/Journal/article/view/12.2> on Oct. 2020. DOI:10.3969/j.issn.1673-923X.2014.03.012
- Man, Z., Sun, L., Hu, H., and Zhang, Y. 2019. Prediction Model of the Spread Rate of Eight typical Surface Dead Fuel in Southern China under Windless and Flat Land. *Scientia Silvae Sinicae*. 55 (7):197-204. DOI: 10.11707/j.10017488.20190722.
- Pan, D., Zhang, H., Pan, G., Yi, L. 2017. Research on masson pine potential fire behavior in southern subtropical based on Behave Plus. *Journal of Central South University of Forestry and Technology*. 37 (06):14-23. DOI:10.14067/j.cnki.1673-923x.2017.06.003.
- Prince D., Shen C., Fletcher T. 2017. Semi-empirical model for fire spread in shrubs with spatially-defined fuel elements and flames. *Fire Technology*, 53 (3):1-31. DOI:10.1007/s10694-016-0644-9.
- Rios, O., Pastor, E., Valero, M. M., and Planas, E. 2016. Short-term fire front spread prediction using inverse modelling and airborne infrared images. *International Journal of Wildland Fire*, 25(10):1033-1047. DOI:10.1071/WF16031
- Rossi, L., Molinier, T., Akhloufi, M., Pieri, A., and Tison, Y. 2013. Advanced stereovision system for fire spreading study. *Fire safety journal*, 60:64-72. DOI: 10.1016/j.firesaf.2012.10.015.
- Viegas, D. X., Almeida, M., Miranda, A. I., and Ribeiro, L. M., 2010. Linear model for spread rate and mass loss rate for mixed-size fuel beds. *International Journal of Wildland Fire*, 19(5):531-540. DOI: 10.1071/WF09007.
- Dahl, N., Xue, H., Hu, X., and Xue, M. 2015. Coupled fire-atmosphere modeling of wildland fire spread using DEVS-FIRE and ARPS. *Natural Hazards*, 77(2):1013-1035. DOI:10.1007/s11069-015-1640-y.
- Ying, L., Han, J., Du, Y., and Shen, Z. 2018. Forest fire characteristics in China: Spatial patterns and determinants with thresholds. *Forest ecology and management*, 424:345-354. DOI:10.1016/j.foreco.2018.05.020.
- Yang, Z., Zhang, H., Zhang, L., and Chen, H. 2018. Experimental study on downslope fire spread over a pine needle fuel bed. *Fire technology*, 54(6):1487-1503. DOI:10.1007/s10694-018-0740-0.
- Zhong, Z., Huang, W., and Li, S. 2017. Forest fire spread simulating model using cellular automaton with extreme learning machine. *Ecological Modelling*. 348(12):33-43. DOI:10.1016/j.ecolmodel.2016.12.022.

Zhang, J., Liu, B., and Chu, T. 2012. Fire behavior of ground surface fuels in *Pinus koraiensis* and *Quercus mongolica* mixed forest under no wind and zero slope condition: A prediction with extended Rothermel model Chinese Journal of Applied Ecology. 23(6):1495-1502. DOI:1001-9332(2012)06-1495-08.